Control of transient chaos in tent maps near crisis. I. Fixed point targeting

C. M. Place and D. K. Arrowsmith
Mathematics Research Centre, Queen Mary and Westfield College, University of London, London E1 4NS, United Kingdom
(Received 23 August 1999)

Combinatorial techniques are applied to the symbolic dynamics representing transient chaotic behavior in tent maps in order to solve the problem of Ott-Grebogi-Yorke control to the nontrivial fixed point occurring in such maps. This approach allows ''preimage overlap'' to be treated exactly. Closed forms for both the probability of control being achieved and the average number of iterations to control are derived. The results are discussed in relation to the work of Tél and shed new light on the transition to the control of permanent chaos.

PACS number(s): 05.45.−a

I. INTRODUCTION

A. Background

Interest in the control of chaotic systems has grown rapidly in the last decade, fueled, in part, by the diverse nature of its applications. For instance, Ditto and Munakata [1] reviewed an impressive array of examples from physics (e.g., laser technology, telecommunications), chemistry (e.g., stabilization of chaotic chemical reactions), and biology (e.g., heart arrhythmias, neural networks).

A notable theoretical catalyst, which has initiated a large number of publications on chaos control, is the technique developed by Ott, Grebogi, and Yorke (OGY) [2] for controlling states of a chaotic system onto an unstable fixed or periodic point using only small controls. The OGY strategy is to allow the uncontrolled chaotic orbit to evolve until it reaches a suitable neighborhood of the target (stage 1) and then to apply small controlling perturbations of a system parameter to stabilize the controlled orbit in the vicinity of the target (stage 2).

The OGY method highlights an important difference between the control of chaos and more regular control systems. In the chaotic case the waiting time before a control is applied depends sensitively on the initial point of the orbit, i.e., this crucial parameter of the control process behaves like a random variable. The distribution of this random variable and its average value are clearly of central importance in practical applications. If the waiting time for control to be applied is inordinately long, then the control procedure may be of little practical value.

The literature associated with chaotic control and its applications has been exhaustively reviewed in the recent book by Chen and Dong [3]. It is clear from this source alone that, for the most part, attention has been focused on controlling permanently chaotic systems. However, there is a sparser but more recent literature on transiently chaotic systems. Such systems may well offer important opportunities for control where a permanently chaotic system cannot be realized or maintained. At the heart of this research effort is the work of Tél [4,5].

The additional complication that transient chaos presents is the possibility that orbits can escape from the vicinity of the repellor (and therefore the target) and never return. It follows that, in contrast to permanently chaotic systems, there is a nonzero probability that control will never be achieved. Thus, for transiently chaotic control it is necessary to consider two characteristics of the control process: (i) the probability that control takes place, and (ii) the time to control when it occurs. The present paper studies these characteristics of transient chaos in a family of piecewise linear maps for which exact results can be derived.

Finally, it should be noted that the symbolic techniques used in this work have a physical interpretation within a thermodynamic formalism. For example, the kth order preimages described in Sec. I C are essentially what are referred to as k cylinders in the thermodynamic approach. When $\nu=1$, these sets cover the interval [0,1] and provide a base for its standard topology. For $\nu>1$, the corresponding sets provide a natural neighborhood system of the repelling invariant set. These neighborhoods provide a symbolic approach to the associated transient chaos. Also, many combinatorial generating functions can be formally interpreted as evaluations of sufficiently general partition functions. For example, the formula (3.9) has such an interpretation within a grand canonical ensemble. While the connection with thermodynamics has not been exploited explicitly in the current work, the interested reader should consult the excellent text of Beck and Schlögl [6] for more details of the thermodynamic approach to chaos.

B. The statistical experiment

Tél [4] addressed the problem of using the OGY strategy [2] to control the transient chaos associated with the crisis [7] of the chaotic attractor that occurs in the one-dimensional family of maps

$$x_{k+1}=a-x_k^2, \tag{1.1}$$

when $a=2$. The aim of the control was to stabilize the nontrivial fixed point (x_F) of the map for a slightly greater than 2, where chaotic transients occur. In the process of estimating the average number of iterations before control was achieved, Tél considered a statistical experiment in which a large number of initial points were chosen at random (i.e., according to a uniform distribution) in the support interval and obtained an expression for the frequency of initial points with orbits reaching the OGY target interval I_F (containing

x_F) in less than or equal to n iterations. The work reported here deals with the analysis of this experiment for the case where the right-hand side of Eq. (1.1) is replaced by the generalized tent map

$$T_\nu(x)=\begin{cases} 2\nu x & \text{for } -\infty<x\leqslant\frac{1}{2} \\ 2\nu(1-x) & \text{for } \frac{1}{2}\leqslant x<\infty \end{cases} \tag{1.2}$$

(see [8]). The more familiar tent (or ''triangle'') map [9], which exhibits permanent chaos, corresponds to $\nu=1$: transient chaos occurs for $\nu>1$.

It is important to emphasize that the statistical experiment outlined above refers only to stage 1 of the OGY procedure, in which the dynamics are those of the uncontrolled system. In this paper, as in [4], stage 2 is only relevant in that it links the length of the target interval to the maximum value that the additive control is allowed to take (see Sec. V). Complications associated with stage 2 that may be encountered for nonlinear maps in general (e.g., failure to achieve or maintain control after entering the target interval) do not occur for the piecewise linear tent maps. For example, linear feedback control ensures the existence of a sequence of additive control parameters such that the controlled orbit remains within the target interval. Thus, control is assured when the stage 1 orbit first enters the target interval.

C. Target preimages

Since the initial points are chosen according to a uniform distribution, the probability of selecting a starting point x_0 with orbit that is controlled in less than or equal to n iterations is given by the length (Lebesgue measure) of the subset of points in [0,1] that contribute to this event. Given that control takes place at the first entry of the orbit of x_0 into I_F the required subset of [0,1] consists of points with orbits that make their first entry into I_F in less than or equal to n time steps. Once entry into the control region is achieved, the control is applied and Eq. (1.2) no longer describes the dynamics. Consider $T_\nu^{-k}(I_F)=\{x_0|T_\nu^k(x_0)\in I_F\}$. The map T_ν^k generates 2^k coverings of [0,1] and the domain of each covering contains a single, connected component of $T_\nu^{-k}(I_F)$, which is conveniently referred to as an ''order-k preimage of I_F.'' Figure 1 shows the 2^k disjoint, kth order preimages of a small target interval I_F, for $k=1$ and 2, when $\nu=1+2^{-5}$. It can be seen that, for each k, half of the preimage components are subsets of those of order $(k-1)$. This structure in the preimages of I_F arises from the action of T_ν, which converts each covering of order $(k-1)$ into two coverings of order k, one of which intersects the original order-$(k-1)$ covering. The result is that each order-$(k-1)$ preimage of I_F leads to two order-k preimages, one of which lies inside the original order-$(k-1)$ preimage. A point $x_0\in T_\nu^{-k}(I_F)\cap T_\nu^{-(k-1)}(I_F)$ has an orbit that enters I_F after at most $(k-1)$ iterations and remains there on the kth iteration. Order-k preimages of I_F that contain such points are of no interest at order k in the control problem, because they should have been counted at lower orders. The relevant points in the order-k preimages of I_F are those lying in the set $U_k=T_\nu^{-k}(I_F)\setminus T_\nu^{-(k-1)}(I_F)$, for each $k\geqslant 1$: these are the points with orbits that first enter I_F in exactly k iterations.

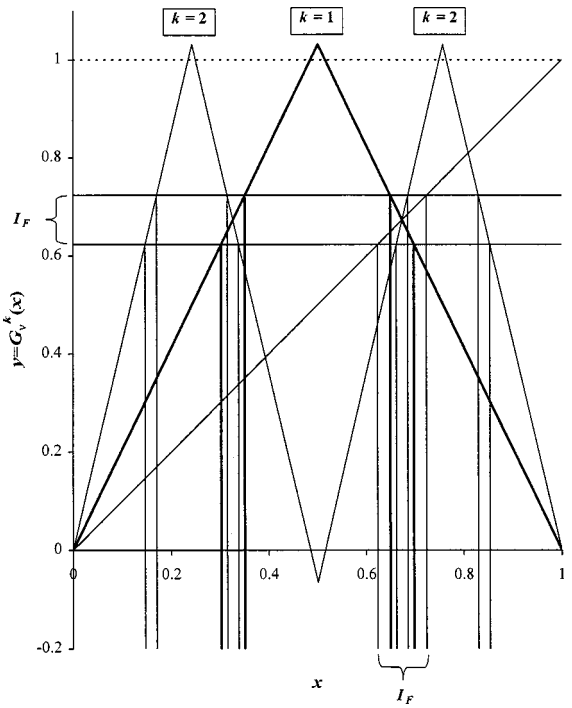

FIG. 1. Illustration of the order-k preimages of a typical target interval I_F under the map (1.2) with $\nu=1+2^{-5}$ and $k=1,2$.

Provided k is not too large, the set U_k is the disjoint union of 2^{k-1} components, each of which is an order-k preimage of I_F. If we choose to denote these ''first-entry'' order-k preimages of I_F by w_{ki}, $i=1,\ldots,2^{k-1}$, then, for $k=1,2,\ldots$,

$$U_k=\cup_{i=1}^{2^{k-1}} w_{ki} \tag{1.3}$$

is the subset of points in [0,1] with orbits that first enter I_F in exactly k iterations of the map (1.2). What is more, since every orbit entering I_F must make its first entry into I_F at a unique value of k, the sets defined in Eq. (1.3) satisfy

$$U_k\cap U_{k-j}=\varnothing \tag{1.4}$$

for $j=1,\ldots,k$, where U_0 is I_F itself. Hence, the set of initial points with orbits that first enter I_F in less than or equal to n iterations is

$$U=\cup_{k=0}^{n} U_k, \tag{1.5}$$

where the union is disjoint because of Eq. (1.4).

D. Preimage overlap

Unfortunately, for given I_F, Eq. (1.3) is valid only provided k is sufficiently small for

$$U_k\cap I_F=\varnothing. \tag{1.6}$$

The domain of the covering of [0,1] generated by T_ν^k that contains the fixed point x_F has nonempty intersection with I_F for all k and, for low k, I_F is typically a proper subset of this domain. Moreover, the 2^{k-1} order-k, first-entry preimages of I_F are disjoint from I_F itself (cf. Fig. 1). However, as k increases, the slope of the covering [equal to $(2\nu)^k$] increases and the length of the domain decreases so that, even-

tually, I_F has nonempty intersection with the domains of adjacent coverings. Inevitably, therefore, there is a value of $k=K$ for which the intersection in Eq. (1.6) first becomes nonempty. A point $x \in U_K \cap I_F$ has the property that $x \in I_F$, $T_\nu^K(x) \in I_F$ but $T_\nu^j(x) \notin I_F$, for $j=1,\ldots,K-1$. The orbit of x starts in I_F, leaves the target interval for $K-1$ iterations, and returns to it at the Kth iteration. All the points of the nonempty ''overlap'' $U_K \cap I_F$ must be excluded from the union in Eq. (1.3). Thus, when such an overlap occurs, Eq. (1.3) is no longer valid, because points in the intersection of the preimage with I_F have been counted already at $k=0$. For $k>K$, the preimages of lower order overlaps must be excluded along with any new overlaps that occur at order k and consequently the size of the overlap grows as k increases above K. Moreover, if $n>K$, overlap has a cumulative effect on the estimate of the set of points that are controlled in less than or equal to n iterations given in Eq. (1.5).

It is apparent from the above discussion that the critical value K is increased if the length of I_F is reduced. Tél [4] avoided the problem of overlap by assuming target interval lengths small enough to maintain the validity of Eq. (1.3) for the values of n considered. In the present work, symbolic dynamics is used to count the number of first-entry preimages of the target interval for any k. This leads to a generalization of Eq. (1.3) and a form for Eq. (1.5) that is valid for any n.

II. SYMBOLIC DYNAMICS FOR TENT MAPS

A. Permanent chaos

For $\nu=1$, the function T_ν, defined in Eq. (1.2), maps $[0,1]$ onto itself, and its non-negative integer powers can be used to associate a binary sequence with each point of $[0,1]$ (cf. [8,9]). The ith element of the sequence, σ_i, is given by

$$\sigma_i = \begin{cases} 0 & \text{if } 0 \leqslant T_\nu^i(x) \leqslant \frac{1}{2} \\ 1 & \text{if } \frac{1}{2} \leqslant T_\nu^i(x) \leqslant 1. \end{cases} \tag{2.1}$$

Equation (2.1) means that for each non-negative integer i, T_1^i (with T_1^0=identity) partitions $[0,1]$ into 2^{i+1} subintervals of equal length, each labeled by a unique symbol block containing $(i+1)$ binary digits. Figure 2(a) illustrates this uniform dissection of $[0,1]$ for $i=0$, 1, and 2. Note that the symbol sequence is built up by appending new binary digits, obtained from Eq. (2.1) for increasing i, to the right-hand end of each symbol block. Thus, the subintervals labeled by the symbol blocks $(.\sigma_0\sigma_1\sigma_2\ldots\sigma_{j-1}0)$ and $(.\sigma_0\sigma_1\sigma_2\ldots\sigma_{j-1}1)$ are both subsets of the subinterval labeled by $(.\sigma_0\sigma_1\sigma_2\ldots\sigma_{j-1})$ and their union covers it. In the limit of i tending to infinity, the subinterval length approaches zero and each resulting infinite binary sequence represents a distinct point in $[0,1]$. Moreover, if x is represented by $(.\sigma_0\sigma_1\sigma_2\ldots)$ then the above construction ensures that $T_1(x)$ corresponds to $(.\sigma_1\sigma_2\ldots)$, i.e., $T_1(x)$ is represented by a left shift on the symbol sequence for x.

It should be noted that points y in $[0,1]$ for which $T_1^k(y)=\frac{1}{2}$, for some non-negative integer k, are not assigned a unique binary sequence by Eq. (2.1). For such points, the binary digits $\sigma_0\ldots\sigma_{k-1}$ are determined by Eq. (2.1) but σ_k can be either 0 or 1. What is more, it is only σ_k that is ambiguous: $\sigma_{k+1}\sigma_{k+2}\ldots=10\ldots$, for all k, because $T_1^{k+1}(y)=1$ and $T_1^{k+j}(y)=0$, for $j=2,3,\ldots$. This indeterminacy [which is a reflection of the ambiguity of the representation of integer multiples of the inverse powers of 2 in base 2, e.g., 1/2 can be represented as $(.100\ldots)$ or $(.011\ldots)$ [9]] is not a serious problem for the symbolic description of the dynamics, but, in relation to the present work, it can be viewed as a remnant of the transient chaotic behavior observed when $\nu>1$ (see Sec. II B). For example, the symbolic representation of the point y described above shows that its orbit can move through $[0,1]$ in an irregular way for $k-1$ iterations before reaching $T_1^k(y)=\frac{1}{2}$ followed by $T_1^{k+1}(y)=1$ and, ultimately, arriving at the fixed point at $x=0$.

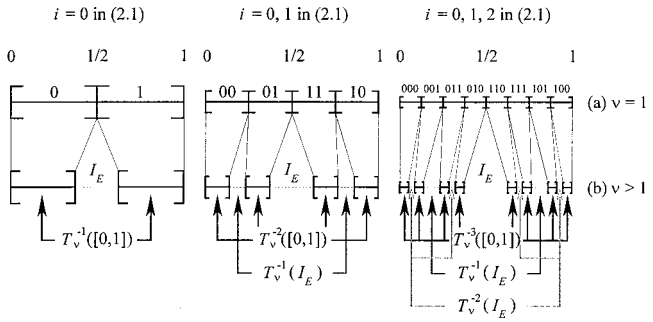

FIG. 2. Illustration of (a) the uniform dissection of [0,1] obtained from non-negative powers of T_1, together with the symbol blocks labeling its subintervals; and (b) the interpretation of the symbol blocks of length k as labels for the order-k preimages of [0,1] under T_ν, for $k=1,2,3$. Note the analogous roles played by the point $x=1/2$ and its preimages when $\nu=1$, and the escape interval I_E and its preimages when $\nu>1$.

B. Transient chaos

For $\nu>1$, T_ν no longer maps $[0,1]$ onto itself, points in the (open) ''escape interval'' $I_E=(\frac{1}{2}[1-(\nu-1)/\nu], \frac{1}{2}[1+(\nu-1)/\nu])$ leave $[0,1]$ under T_ν. An alternative interpretation (equally valid for $\nu=1$) of the coding of the points in $[0,1]$ given by Eq. (2.1) can be obtained by recognizing that, for each positive integer j, the 2^j symbol blocks $(.\sigma_0\sigma_1\sigma_2\ldots\sigma_{j-1})$ uniquely label the (closed) preimages of $[0,1]$ under T_ν^j [see Fig. 2(b)]. This view of the coding emphasizes the correspondence between the symbol blocks and the 2^j coverings of $[0,1]$ generated by T_ν^j. It also makes clear that the ambiguity of the symbolic representation of the preimages of $x=1/2$, for $\nu=1$, arises because the length of the escape interval goes to zero in that case.

As Fig. 2(b) illustrates, the procedure (2.1) attributes a unique symbol block $(.\sigma_0\sigma_1\ldots\sigma_{k-2}\sigma_{k-1})$ of k binary digits (a k block) to each of the order-k preimages of $[0,1]$ that make up the 2^k components of the set of points with orbits that remain in $[0,1]$ for at least k iterations. The remainder of $[0,1]$ is filled out by the preimages of I_E of order $j=0,1,2,\ldots,k-1$. The union of these preimages is the set of points with orbits that enter the escape interval in less than or equal to $k-1$ iterations (i.e., that leave $[0,1]$ in less than or equal to k iterations). It follows that, for each positive integer k, $[0,1]$ is partitioned into I_E and the preimages of I_E of order

less than or equal to $(k-1)$, together with the 2^k components of the set of points with orbits that remain in $[0,1]$ for at least k iterations (i.e., the order-k preimages of $[0,1]$).

It is evident that, in the limit of k tending to infinity, Eq. (2.1) provides symbol sequences only for points with orbits that remain in $[0,1]$ indefinitely. For $\nu>1$, such points are the elements of the Cantor set formed by the deletion of all of the preimages of I_E. For $\nu=1$, I_E has zero length, every point of $[0,1]$ remains in $[0,1]$ indefinitely. Every point is represented by an infinite binary sequence but the preimages of $x=1/2$, where the closed preimages of $[0,1]$ overlap, are not represented uniquely.

It should be noted that, for $\nu>1$, all the features of ''chaotic behavior'' predicted by the conjugacy of T_ν and the left shift on infinite binary sequences (including a dense set of periodic orbits, aperiodic orbits, etc.) occur on the invariant Cantor set described above. It is this repelling invariant set (which has Lebesgue measure zero) that is responsible for the transient chaotic behavior studied here. Each transiently chaotic orbit ultimately escapes from $[0,1]$, i.e., there exists a non-negative integer k such that the initial point x_0 of the orbit lies in an order-k preimage of I_E but does not lie in any order-j preimage of that interval with $j<k$. It follows that the orbit of x_0 remains in $[0,1]$ for k iterations, entering I_E on the kth step, and Eq. (2.1) provides a binary symbol block $(.\sigma_0\sigma_1\ldots\sigma_{k-2}\sigma_{k-1})$ based on the evolution of this part of the orbit. This block determines the order-k preimage of $[0,1]$ containing x_0 and, under left shift, the order-$(k-j)$ preimage of $[0,1]$ containing $T_\nu^j(x_0)$ for $j=1,\ldots,k-1$. It is important to distinguish the finite symbol blocks that are used in this symbolic treatment of transient chaotic behavior from the infinite symbol sequences that describe the permanent chaos that takes place on the invariant Cantor set.

III. A SYMBOLIC APPROACH TO OTT-GREBOGI-YORKE CONTROL

A. Target intervals

It is easily verified that the symbol sequence corresponding to the nontrivial fixed point of T_ν is $(.111\ldots)$. The relationship between symbol blocks of increasing length (see Sec. II) means that this point lies inside every member of the sequence of subintervals of $[0,1]$ represented by $\{(.1),(.11),(.111),\ldots\}$. In order to make use of symbolic dynamics in the control of transient chaos it is necessary to take the target interval I_F to be one of these subintervals. This means that some flexibility in the choice of I_F must be sacrificed and the luxury of having the fixed point centrally placed in I_F has to be given up. However, the target intervals defined by symbolic dynamics have significant advantages over other choices in that (a) partial overlap of the preimages of I_F with I_F itself does not occur, and (b) established combinatorial methods (associated with finite binary strings) can be used to count the number of first-entry preimages present at any order.

B. Characterization of first-entry preimages

Suppose that I_F is taken to be the interval labeled by the r block $(.11\ldots1)_r$, where the subscript indicates the number of digits in the block. Recall from Sec. I that the aim is to obtain the number of preimages of I_F containing points with orbits that first enter I_F in less than or equal to n iterations. The preimages of I_F of order k are represented by symbol blocks derived from $(.11\ldots1)_r$, by appending k binary digits to its left-hand end. The resulting $(k+r)$ block, $(.\sigma_1\sigma_2\ldots\sigma_k11\ldots1)_{k+r}$, clearly yields $(.11\ldots1)_r$ after k successive applications of a left shift. All 2^k such preimage blocks represent subintervals of $[0,1]$ containing points with orbits that enter I_F after k iterations, but only those for which this is the first entry into I_F are to be counted. Such preimage symbol blocks are distinguished by the property that the binary string $\sigma_1\sigma_2\ldots\sigma_k11\ldots1$ of length $k+r$ contains the substring consisting of r adjacent 1's, at its right-hand end but nowhere else within it. $\sigma_{j+1}=\sigma_{j+2}=\ldots=\sigma_k=1$ then the orbit of points in this preimage would enter I_F after $j<k$ iterations, so that the entry occurring after k iterations would not be the first.

C. Combinatorics for characteristic strings

The problem of counting binary strings with a given substring occurring only at one end has been dealt with by Odlyzko [10]. The calculation, for the case of interest here, may be outlined as follows. Let A denote the binary string of r adjacent 1's and define (a) $f_A(m)$ to be the number of binary strings of length m that do not contain A (as a substring of r adjacent binary digits) anywhere within them; and (b) $g_A(m)$ to be the number of binary strings of length m with the property that A occurs at the right-hand end but nowhere else within them. Note that $g_A(m)=0$, for $m=0,1,\ldots,r-1$, because there can be no binary strings of length less than r that have A at their right-hand end.

If $B=(b_1b_2\ldots b_m)$ does not contain A as a connected substring then $Bb=(b_1b_2\ldots b_mb)$, with $b=0,1$, must either fail to contain A anywhere or contain A only at its right-hand end. Thus

$$2f_A(m)=f_A(m+1)+g_A(m+1). \tag{3.1}$$

Furthermore, each concatenation BA contains A in one, and only one, of the forms

$$\begin{aligned} BA&=(b_1b_2\ldots b_j\overbrace{11\ldots1}^{r}\overbrace{11\ldots1}^{m-j})\\ &=(b_1b_2\ldots b_jA\overbrace{11\ldots1}^{m-j}), \end{aligned} \tag{3.2}$$

with $j=m,m-1,m-2,\ldots,m-r+1$. The leftmost substring of length $j+r$ in Eq. (3.2) has A at its right-hand end but nowhere else within it: the number of such strings is $g_A(j+r)$. Since the total number of concatenations BA is $f_A(m)$, it follows that

$$f_A(m)=\sum_{j=m-r+1}^{m} g_A(j+r)=\sum_{i=1}^{r} g_A(m+i). \tag{3.3}$$

Equations (3.1) and (3.3) can be used to obtain both a recurrence relation and a generating function for the numbers $g_A(m)$. The recurrence relation,

$$g_A(m+r+1)=\sum_{j=0}^{r-1} g_A(m+r-j), \tag{3.4}$$

follows when Eq. (3.3) is used to eliminate $f_A(m)$ and $f_A(m+1)$ from Eq. (3.1). The generating function can be obtained as follows. Multiplication of Eqs. (3.1) and (3.3) by z^m and summation from m equals zero to infinity yields, respectively,

$$2F_A(z)=z^{-1}(F_A(z)-1)+z^{-1}G_A(z), \tag{3.5}$$

and

$$F_A(z)=z^{-r}C_A(z)G_A(z), \tag{3.6}$$

where

$$C_A(z)=\sum_{i=0}^{r-1} z^i. \tag{3.7}$$

In Eqs. (3.5)–(3.7), $F_A(z)$ and $G_A(z)$ are the generating functions for $f_A(m)$ and $g_A(m)$, respectively, and $C_A(z)$ is the correlation polynomial for the binary string A (see Odlyzko [10]). Equation (3.5) can be written in the form

$$(1-2z)F_A(z)+G_A(z)=1 \tag{3.8}$$

and substitution of Eq. (3.6) gives

$$G_A(z)=\sum_{m=0}^{\infty} g_A(m)z^m=\frac{z^r}{[z^r+(1-2z)C_A(z)]}$$

$$=\frac{z^r}{\left(1-\sum_{i=1}^{r} z^i\right)}. \tag{3.9}$$

D. Numbers of first-entry preimages of I_F

Since $(.11\ldots1)_r$ represents the target interval I_F, the number $g_A(m)$ of binary strings of length m that have the substring A at their right-hand end, but nowhere else, is equal to the number $N_k^{(r)}$ of preimages of I_F of order $k=m-r$ containing points with orbits that first enter I_F after k iterations of the tent map. Thus $N_k^{(r)}=g_A(k+r)$ and the recurrence relation (3.4) becomes

$$N_{k+1}^{(r)}=\sum_{j=0}^{r-1} N_{k-j}^{(r)}. \tag{3.10}$$

Recognizing that $g_A(m)=0$ for $m=1,\ldots,r-1$ is equivalent to $N_{-j}^{(r)}=0$, $j=1,\ldots,r-1$ and noting that $g_A(r)=N_0^{(r)}=1$, Eq. (3.10) provides an efficient algorithm for generating the numbers $N_k^{(r)}$. For $r=2$, Eq. (3.10) leads to the Fibonacci numbers.

Observe that Eq. (3.10) gives $N_k^{(r)}=2^{k-1}$, for $k=1,\ldots,r$, and $N_{k+1}^{(r)}=2^r-1$, showing that the preimage ''overlap'' referred to by Tél [4] first occurs for $k=r+1$. This result is immediately apparent from the symbolic approach. The first-order preimages of I_F are represented by $(.011\ldots1)_{r+1}$ and $(.111\ldots1)_{r+1}$. The latter preimage clearly lies within I_F, as do all its preimages, resulting in only half of the preimages of I_F satisfying the first entry condition in any order. What is more, the preimages of I_F up to order r arising from $(.011\ldots1)_{r+1}$ can only contain a binery string of r adjacent 1's at their right-hand end, and therefore all 2^{k-1} of these preimages contribute for $k=1,\ldots,r$. One preimage of order $r+1$, namely, that represented by $(.11\ldots1011\ldots1)_{2r+1}$, fails to satisfy the first-entry condition, so that $N_{r+1}^{(r)}=2^r-1$.

The generating function $\hat{G}_r(z)$ for the numbers $\{N_k^{(r)}\}_0^\infty$ can be obtained from Eq. (3.9) by, once again, remembering that $g_A(m)=0$, for $m=0,1,\ldots,r-1$. Thus

$$G_A(z)=\sum_{m=r}^{\infty} g_A(m)z^m=z^r\sum_{k=0}^{\infty} N_k^{(r)}z^k=z^r\hat{G}_r(z), \tag{3.11}$$

where

$$\hat{G}_r(z)=\sum_{k=0}^{\infty} N_k^{(r)}z^k=\left(1-\sum_{i=1}^{r} z^i\right)^{-1}. \tag{3.12}$$

IV. CALCULATION OF PROBABILITIES

In the context of the statistical experiment described in Sec. I, the probability with which points, chosen according to a uniform distribution in [0,1], will be controlled in less than or equal to n iterations is given by the sum of the lengths of the first-entry preimages of I_F of order less than or equal to n. The length of the target interval I_F represented by $(.11\ldots1)_r$ is $(2\nu)^{-r}$ and the lengths of the preimage intervals of order k are all equal and given by $(2\nu)^{-r}(2\nu)^{-k}$. Hence the probability of choosing an initial point with an orbit that first enters I_F in exactly k iterations is $N_k^{(r)}(2\nu)^{-(k+r)}$ and the probability of selecting an initial point that is controlled in less than or equal to n iterations of the map T_ν is

$$p_n(\nu,r)=(2\nu)^{-r}\sum_{k=0}^{n} N_k^{(r)}(2\nu)^{-k}. \tag{4.1}$$

In the limit of n tending to infinity, the summation in Eq. (4.1) becomes the generating function $\hat{G}_r(z)$ evaluated at $(2\nu)^{-1}$ and the probability that control is ultimately achieved is given by

$$p(\nu,r)=\lim_{n\to\infty}\{p_n(\nu,r)\}=(2\nu)^{-r}\hat{G}_r((2\nu)^{-1})=G_A((2\nu)^{-1}). \tag{4.2}$$

Substitution of $\hat{G}_r(z)$ from Eq. (3.12) yields

$$p(\nu,r)=\frac{(2\nu-1)}{(2\nu)^r(2\nu-2)+1}. \tag{4.3}$$

Since Eq. (4.1) is a sum of positive terms, this limiting value represents an upper limit to the probability of successful control for given ν and r.

A. Permanent chaos ($\nu=1$)

In this case, the whole of the interval [0,1] is a chaotic invariant set for T_1. The set of points in [0,1] corresponding to symbol sequences that contain every finite symbol block at least once has measure 1 [8,11]. This means that, with probability 1, the orbits of all choices of initial point in [0,1] will eventually pass through the target interval I_F. Hence the measure of initial points whose orbits first enter I_F in less than or equal to n iterations must tend to unity as n tends to infinity. This limiting behavior is confirmed by the expression for $p(\nu,r)$ in Eq. (4.3) which reduces to unity for $\nu=1$.

B. Transient chaos ($\nu>1$)

In contrast to Sec. IV A, when $\nu>1$, the measure of the initial points with orbits that ultimately remain in [0,1] is zero. Every point x_0 in the complement of the invariant Cantor set must therefore belong to a preimage of I_E of some order k, with $k\geqslant 0$. However, every preimage of order k of I_E is a subinterval of the corresponding preimage of [0,1] of order k (see Sec. II). For $k\geqslant 1$, the latter is labeled by a binary symbol block $(.\sigma_0\sigma_1\ldots\sigma_{k-1})$ and the evolution of the points within it is given by applying successive left shifts to this block. After $k-1$ iterations, $T_\nu^{k-1}(x_0)$ lies in the subinterval represented by $(.\sigma_{k-1})$ and enters the escape interval at the next iteration. If the orbit of x_0 enters I_F then r adjacent 1's must occur as a connected substring within $\sigma_0\sigma_1\ldots\sigma_{k-1}$. Conversely, if $\sigma_0\sigma_1\ldots\sigma_{k-1}$ does not contain this substring, then the orbit of x_0 enters I_E after k iterations without entering I_F. The orbit of such a point will never be controlled for it will subsequently leave [0,1] and not return. The number of binary strings of length k that do not contain a substring of r adjacent 1's anywhere within them is $f_A(k)$ and each of the corresponding symbol blocks represents a subinterval of [0,1] containing a preimage of I_E of length $(1-\nu^{-1})(2\nu)^{-k}$. Thus the probability of selecting an initial point with an orbit that enters I_E in less than or equal to n iterations, without passing through I_F, is

$$\overline{p_n}(\nu,r)=(1-\nu^{-1})\sum_{k=0}^{n} f_A(k)(2\nu)^{-k}. \tag{4.4}$$

In the limit of n tending to infinity, Eq. (4.4) becomes

$$\overline{p}(\nu,r)=\lim_{n\to\infty}\{\overline{p_n}(\nu,r)\}=[(1-2z)F_A(z)]_{z=(2\nu)^{-1}}. \tag{4.5}$$

The sequence $\{\overline{p_n}(\nu,r)\}_{n=0}^{\infty}$ is increasing, so that $\overline{p}(\nu,r)$ is an upper bound for $\overline{p_n}(\nu,r)$. The form of the generating function $F_A(z)$ given in Eqs. (3.6) and (3.7) can be used [along with Eqs. (3.11) and (3.12)] to show that

$$F_A(z)=\sum_{k=0}^{\infty}\left(\sum_{i=0}^{r-1} N_{k-i}^{(r)}\right)z^k. \tag{4.6}$$

It then follows from the recurrence relation (3.10) that

$$f_A(k)=N_{k+1}^{(r)}. \tag{4.7}$$

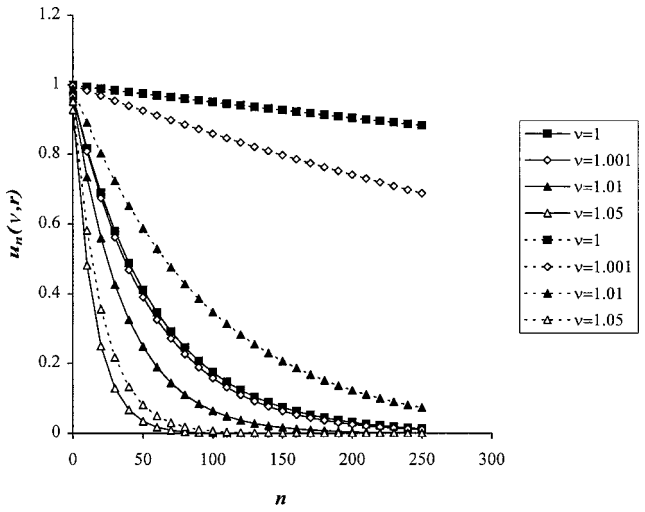

FIG. 3. Plots of $u_n(\nu,r)$ for ν=1,1.001,1.01,1.05 when $r=5$ (solid line); and $r=10$ (dashed line). The stronger r dependence of $u_n(1,r)$ compared with $u_n(1.05,r)$ arises because the former is determined by the convergence of $p_n(1,r)$ to 1, while the latter is dominated by the convergence of $\overline{p_n}(1.05,r)$ to $\overline{p}(1.05,r)$. A discussion of $u_n(\nu,r)$ and its relation to the design of numerical experiments can be found in [12].

Thus Eq. (3.10) provides a convenient way of obtaining the data necessary to evaluate the finite summations in both Eqs. (4.1) and (4.4).

C. Numerical results

Calculations of $p_n(\nu,r)$ and $\overline{p_n}(\nu,r)$ reveal that their sum is less than unity. This is to be expected, since there are points in [0,1] with orbits that do not satisfy the requirements assumed in deriving either Eq. (4.1) or Eq. (4.4). In other words, there are initial points with orbits that fail to reach either I_E or I_F in less than or equal to n iterations. Thus, for any finite n, there is a nonzero probability $u_n(\nu,r)$ that the fate of the initial point is undecided after n iterations. However, every point of [0,1] must belong to one, and only one, of three mutually exclusive possibilities: (a) its orbit enters I_F; (b) its orbit reaches I_E, without entering I_F; or (c) its orbit fails to reach either I_F or I_E; in less than or equal to n iterations. Therefore,

$$p_n(\nu,r)+\overline{p_n}(\nu,r)+u_n(\nu,r)=1. \tag{4.8}$$

As n tends to infinity, $u_n(\nu,r)$ must go to zero (cf. Fig. 3). This follows because almost all (in the sense of Lebesgue measure) initial points in [0,1] have orbits that ultimately leave that interval and each such orbit either passes through I_F or it does not. Therefore, the sum of the limiting forms given in Eqs. (4.2) and (4.5) must be unity. Substitution of Eqs. (4.2) and (4.5) into Eq. (3.8) shows that

$$p(\nu,r)+\overline{p}(\nu,r)=1, \tag{4.9}$$

for any choice of the positive integer r or $\nu\geqslant 1$. Notice also that Eqs. (4.8) and (4.9) imply

$$u_n(\nu,r)=[p(\nu,r)-p_n(\nu,r)]+[\overline{p}(\nu,r)-\overline{p_n}(\nu,r)]. \tag{4.10}$$

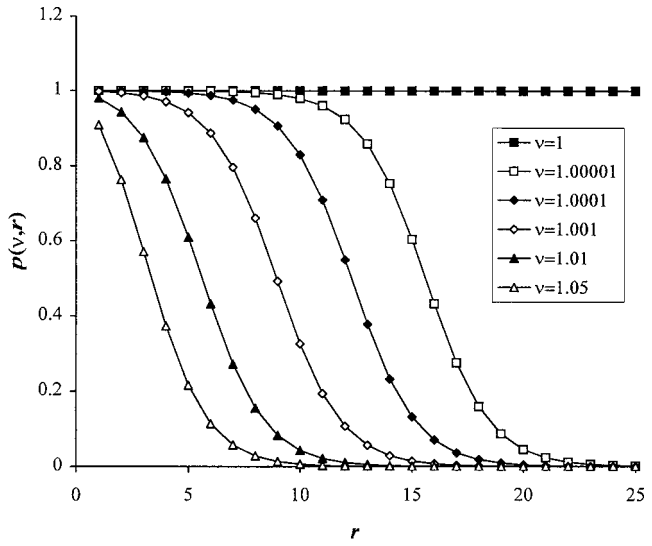

FIG. 4. Numerical illustration of the dependence of $p(\nu,r)$ on ν and r. Plots of p as a function of r are shown for trial values of ν.

The first term in Eq. (4.10) represents the maximum increase in the probability of successful control that can be achieved by increasing n. For given ν and r, no matter how large n becomes, there remains a probability $\overline{p}(\nu,r)=1-p(\nu,r)$ that control will not be achieved.

Numerical values of $p(\nu,r)$ for some trial values of ν and r are given in Fig. 4. Observe that, for all of the trial values of $\nu>1$, $p(\nu,r)$ falls to a value close to zero for $r\approx 20$, but the closer ν is to 1 the longer $p(\nu,r)$ remains near to unity. Recall that the length of I_F is $(2\nu)^{-r}\leqslant 2^{-r}$, so that, for the values of $\nu>1$ in Fig. 4, the probability of successful control has all but vanished for target intervals of length approximately equal to 10^{-6}. Hence, control problems that impose the use of small target interval lengths, while ν is bounded away from 1, must be treated with caution if a realistic probability of successful control is to be maintained.

V. AVERAGE NUMBER OF ITERATIONS TO CONTROL

A. The assumption of controllability

It can be argued that a practical estimate of the average number of iterations to be involved in a numerical experiment should take account of the iterations that occur in failed runs, i.e., initial points with orbits that fail to reach the target interval in the maximum number n_* of iterations allowed. In this context, any orbit that fails to reach the target interval in n_* iterations must be counted as a failure. The probability of choosing such an initial point is $1-p_{n_*}(\nu,r)=\overline{p}_{n_*}(\nu,r)+u_{n_*}(\nu,r)$. As Fig. 4 shows, $p(\nu,r)$ [and hence $p_{n_*}(\nu,r)$] can be significantly different from unity and, in such cases, failure to achieve control would make an additional contribution of $n_*[1-p_{n_*}(\nu,r)]$ to the expected number of iterations involved in the experiment. For $\nu>1$, this contribution diverges as $n_*\to\infty$. In order to avoid this difficulty, the calculation of the average number of iterations required for control to take place makes use of the conditional probability distribution that assumes control actually occurs.

It follows that the average number of iterations to control is a property of the set of controllable points, while the probability that control takes place is a property of the set of initial points as a whole. Information about the failure to achieve control is embodied in the latter. When designing a numerical experiment both properties must be considered. Clearly, it is advisable to arrange for $p_{n_*}(\nu,r)$ to be close to 1, in order to avoid wasting computer resources on failed runs. For example, a possible strategy might be to choose (a) r so that the length of the target interval is compatible with the maximum control parameter; (b) ν so that $p(\nu,r)$ is sufficiently close to unity; and (c) n_* so that $u_{n_*}(\nu,r)$ is close to zero. However, although such precautions ensure that the experiment ''hit rate'' is sufficiently close to 1, they reveal nothing of the number of time steps that have to be made before the target interval is reached when control does take place.

B. Calculation of the conditional average

For those initial points with orbits that are controlled, the number of iterations required to reach the target interval is a random variable. If the target interval I_F is represented by the code block $(.11\ldots1)_r$, the probability of selecting an initial point that first reaches I_F in exactly k iterations is $N_k^{(r)}(2\nu)^{-(k+r)}$. It then follows (cf. Tél [4]) that the average number of time steps to control, $\tau(\nu,r)$, is given by

$$\tau(\nu,r)=\frac{(2\nu)^{-r}\sum_{k=1}^{\infty}kN_k^{(r)}(2\nu)^{-k}}{(2\nu)^{-r}\sum_{k=0}^{\infty}N_k^{(r)}(2\nu)^{-k}}. \tag{5.1}$$

Observe that Eq. (5.1) involves only initial points with orbits that reach I_F. It is therefore an average with respect to the conditional probability distribution, which assumes that control occurs.

The generating function $\hat{G}_r(z)$ obtained in Sec. III can be used to evaluate the sums appearing in Eq. (5.1). It can be shown that

$$\tau(\nu,r)=\left[\frac{z\hat{G}_r'(z)}{\hat{G}_r(z)}\right]_{z=(2\nu)^{-1}}, \tag{5.2}$$

where $'$ denotes differentiation with respect to z, and substitution of Eq. (3.12) yields the result

$$\tau(\nu,r)=\left[\frac{z\{1-(r+1)z^r+rz^{r+1}\}}{(1-z)\{1-2z+z^{r+1}\}}\right]_{z=(2\nu)^{-1}}. \tag{5.3}$$

C. Limiting behavior of $\tau(\nu,r)$ for small target intervals

To examine the behavior of $\tau(\nu,r)$ near the crisis at $\nu=1$, it is convenient to write $(2\nu)^{-1}=2^{-1}(1-\delta)$, so that Eq. (5.3) becomes

$$\tau(\nu,r)=\left(\frac{1-\delta}{1+\delta}\right)\times\left[\frac{1-(r+1)2^{-r}(1-\delta)^r+r2^{-(r+1)}(1-\delta)^{r+1}}{\delta+2^{-(r+1)}(1-\delta)^{r+1}}\right]. \tag{5.4}$$

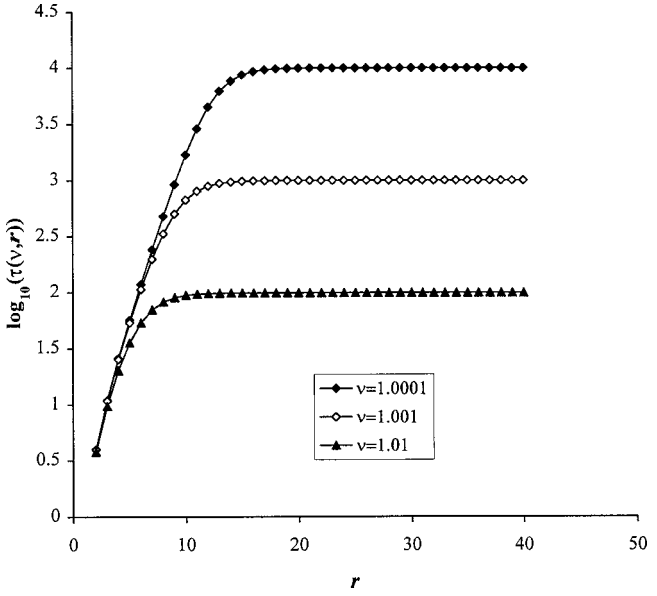

FIG. 5. Plots of $\tau(\nu,r)$ calculated using Eq. (5.3) for $\nu=1.01$, 1.001, and 1.0001. The limiting values obtained agree with those given by Eq. (5.5). Note that the base-10 logarithm of $\tau(\nu,r)$ is plotted, rather than $\tau(\nu,r)$ itself, in order to present the data on a single graph.

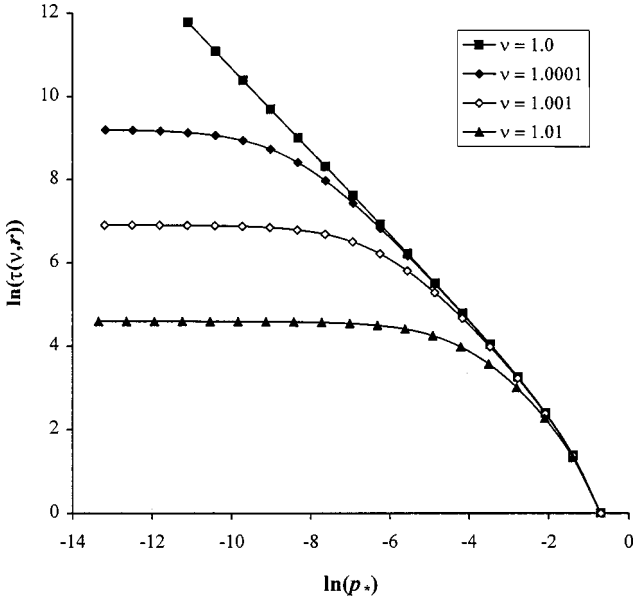

FIG. 6. Plots of $\ln[\tau(\nu,r)]$ as a function of $\ln(p_*)$ obtained from Eq. (5.3) for $\nu=1.01$, 1.001, 1.0001, and 1.0. Note that the graph for $\nu=1$ has slope -1 for small enough p_* as predicted by Eq. (5.10).

For given $0<\delta<1$, the terms containing factors of 2^{-r} are negligible compared with δ for sufficiently large r, and

$$\tau(\nu,r)\approx\left(\frac{1-\delta}{1+\delta}\right)\frac{1}{\delta}=\tau_\infty(\nu). \tag{5.5}$$

Thus $\tau(\nu,r)$ becomes essentially independent of r when r is large enough (see Fig. 5), i.e., it is essentially independent of the length of the target interval when the latter is sufficiently small (cf. Tél [4]). For δ tending to zero, i.e., very close to crisis, Eq. (5.5) gives

$$\tau_\infty(\nu)\approx\frac{1}{\delta}. \tag{5.6}$$

By definition $\delta=(1-\nu^{-1})$, so that $-\ln\nu=\ln(1-\delta)\approx-\delta$ and

$$\tau_\infty(\nu)\approx\frac{1}{\ln\nu}. \tag{5.7}$$

The escape rate κ is defined (cf. Tél [13]) in terms of the asymptotic form $W_n\sim\exp(-\kappa n)$ of the probability W_n that a randomly chosen point has not escaped from [0,1] after n iterations. Direct summation of the lengths of the preimages of the escape interval shows that $W_n=\nu^{-n}=\exp(-n\ln\nu)$ for the orbits of T_ν, so that $\kappa=\ln\nu$. Thus Eq. (5.7) can be written as

$$\tau_\infty(\nu)\approx\frac{1}{\kappa}, \tag{5.8}$$

in agreement with Tél [4]. It is important to note that the forms given in Eqs. (5.5)–(5.8) are not valid when $\delta=0$ (or, equivalently, if $\nu=1$ or $\kappa=\ln\nu=0$); rather, Eq. (5.4) then gives

$$\tau(1,r)=\frac{1-(r+1)2^{-r}+r2^{-(r+1)}}{2^{-(r+1)}}\approx\frac{2}{l(I_F)}, \tag{5.9}$$

for sufficiently large values of r. Here $l(I_F)=(2\nu)^{-r}$ is the length of the target interval, so that Eq. (5.9) shows that $\tau(1,r)$ diverges as r tends to infinity because the length of the target interval tends to zero. In the OGY method the length of the target interval is usually determined by the maximum allowed value of the control parameter p_*. A straightforward calculation for the control in stage 2 yields $p_*=\nu l(I_F)$ for the map T_ν, so that Eq. (5.9) gives

$$\tau(1,r)\approx\frac{2}{p_*}, \tag{5.10}$$

when r is large enough (cf. Tél [4]). Clearly, a similar expression to Eq. (5.9) holds when $\delta>0$ but is small compared to $(2\nu)^{-r}$. In such situations, a transition between the limiting forms given in Eqs. (5.8) and (5.10) takes place as r is increased with δ held fixed. This transition is illustrated in Fig. 6. Following Tél (cf. Fig. 4 of [4]), plots of $\ln[\tau(\nu,r)]$ as a function of $\ln(p_*)=\ln[\nu(2\nu)^{-r}]$ are shown, so that the limiting slope of -1 predicted by Eq. (5.10) is visible for $\nu=1$.

VI. ROLE OF PREIMAGE ORDERS WITHOUT OVERLAP

It was shown in Sec. III that overlap (as defined in Sec. I) affects the number of preimages of the target interval only at orders greater than r. Since $N_0^{(r)}=1$, $N_k^{(r)}=2^{k-1}$ for $k=1,\ldots,r$, Eq. (4.1) can be written in the alternative form

$$p_n(\nu,r)=(2\nu)^{-r}\left(1+\frac{1}{2\nu}\sum_{j=0}^{r-1}\nu^{-j}+\sum_{k=r+1}^{n}N_k^{(r)}(2\nu)^{-k}\right), \tag{6.1}$$

when $n>r$. For n less than or equal to r, only the first summation in Eq. (6.1) appears. These terms, where the number

of first-entry preimages is unaffected by overlap, were used by Tél [4] as the basis of his treatment of τ. The aim of this section is to discuss the significance of these ''nonoverlap'' terms for the tent maps (1.2).

A. Approximation of the distribution $p(\nu,r)$

When the target interval is represented by the code block $(.11\ldots1)_r$, there are no effects of preimage overlap for $n \leqslant r$. The approach taken by Tél [4] is to assume that n is sufficiently small for no overlap to occur for the target interval chosen. In the following discussion it will be assumed that, for the given symbolic target interval, n is the largest value for which this is true, namely, $n=r$, and define

$$\tilde{p}(\nu,r)=(2\nu)^{-r}\left(1+\frac{1}{2\nu}\sum_{j=0}^{r-1}\nu^{-j}\right). \tag{6.2}$$

It is always the case that $\tilde{p}(\nu,r)<p(\nu,r)$, but for what values of r (i.e., for what target interval lengths) does the former provide a reasonable approximation to the latter? The sum of the geometric progression in Eq. (6.2) can be written as

$$\tilde{p}(\nu,r)=\begin{cases}(2\nu)^{-r}\dfrac{2(\nu-1)+1-\nu^{-r}}{2(\nu-1)}, & \nu>1\\[2ex] 2^{-r}\dfrac{2+r}{2}, & \nu=1,\end{cases} \tag{6.3}$$

while a minor rearrangement of Eq. (4.3) gives

$$p(\nu,r)=\begin{cases}(2\nu)^{-r}\dfrac{2(\nu-1)+1}{2(\nu-1)+(2\nu)^{-r}}, & \nu>1\\[2ex] 1, & \nu=1.\end{cases} \tag{6.4}$$

In order to compare Eqs. (6.3) and (6.4) when $\nu>1$, consider

$$\frac{\tilde{p}(\nu,r)}{p(\nu,r)}=\left[\frac{2(\nu-1)+1-\nu^{-r}}{2(\nu-1)+1}\right]\left[\frac{2(\nu-1)+(2\nu)^{-r}}{2(\nu-1)}\right]. \tag{6.5}$$

It is convenient to write $\nu-1=\epsilon$, where ϵ is typically positive, less than 1 and tends to zero as the crisis is approached from above. It then follows that

$$\begin{aligned}\frac{\tilde{p}(\nu,r)}{p(\nu,r)}&=1-\frac{(1+\epsilon)^{-r}}{(1+2\epsilon)}+\frac{2^{-r}(1+\epsilon)^{-r}}{2\epsilon}\left\{1-\frac{(1+\epsilon)^{-r}}{(1+2\epsilon)}\right\}\\&=1-\eta(r,\epsilon),\end{aligned} \tag{6.6}$$

where η is the relative error in $\tilde{p}(\nu,r)$. The presence of a factor of ϵ^{-1} in the second term of η shows that care must be taken if the crisis is to be approached closely. It is possible to suppress this term by increasing r, because of the factor of 2^{-r} that occurs in its numerator. However, the first term of η remains a problem unless either ϵ is significantly different from zero or r is large enough to reduce $(1+\epsilon)^{-r}$ to an acceptable value. An estimate of the value of r required to achieve a given relative error when ϵ is very close to zero can be obtained as follows. It can be shown that if r is such that $(1+\epsilon)^{-r}\ll 1$ then $2^{-(r+1)}\ll\epsilon$ and the first term of η is dominant. Thus, since ϵ is close to zero, $\eta\approx(1+\epsilon)^{-r}$ implies

$$r\approx\frac{-\ln(\eta)}{\ln(1+\epsilon)}\approx\frac{-\ln(\eta)}{\epsilon}. \tag{6.7}$$

The values of r given by Eq. (6.7) indicate that $\tilde{p}(\nu,r)$ cannot provide a realistic approximation to $p(\nu,r)$ in any practical situation. For example, given the modest requirement that $\eta=e^{-3}\approx0.05$, Eq. (6.7) gives $r=300$ for $\epsilon=0.01$ and $r=3000$ for $\epsilon=0.001$. In the former case, this means that

$$\tilde{p}(\nu,r)\sim p(\nu,r)\sim(2\nu)^{-r}\left\{1+\frac{1}{2\epsilon}\right\}\approx10^{-90}, \tag{6.8}$$

while in the latter case the asymptotic form given in Eq. (6.8) is of order 10^{-900}. In terms of the statistical experiment of Sec. I, there is essentially no probability of control in such cases because the target interval length is so small for such values of r.

In conclusion, therefore, while $\tilde{p}(\nu,r)$ and $p(\nu,r)$ both have the same asymptotic form [namely, that given in Eq. (6.8)] as r tends to infinity, the value of r required to satisfy comparatively modest constraints on the relative error η increases rapidly as ν decreases toward unity. Indeed, the approximation afforded by the contribution arising from preimages without overlap in Eq. (6.1) is of no practical value for $\epsilon=\nu-1\leqslant0.01$, because the probability of successful control is essentially zero for target intervals small enough to avoid preimage overlap.

When ϵ is somewhat greater, acceptable values of the relative error η can be obtained for more realistic target interval lengths [e.g., for $\epsilon=0.2$, $\eta=0.05$, Eq. (6.7) gives $r\approx15$ and Eq. (6.8) yields $p(\nu,r)\approx10^{-5}$]. This is a reflection of the reduced significance of overlap when ν is substantially greater than 1. The length of each order-k preimage of I_F is $(2\nu)^{-(k+r)}$ and this is smaller the greater the value of ν. The corrections arising from overlap, which first appear for $k=r+1$, are therefore of smaller magnitude when ν is substantially greater than one. When $\nu=1$, the total length of the pre-images of order k (in the absence of overlap) is $2^{-(r+1)}$, independent of k, and, when n tends to infinity with a target interval of finite length, overlap is the mechanism whereby divergence of the sum appearing in Eq. (4.1) is avoided. Thus overlap plays an essential role in the treatment of the control problem when $\nu=1$.

B. Overlap corrections to the probability density function

The increase in the significance of overlap as ν approaches 1 is apparent in the probability density function $P(\nu,r;k)$ for $p(\nu,r)$, where the terms with and without overlap occur in different ranges of k.

The probability density function corresponding to the distribution $p(\nu,r)$ is given by

$$P(\nu,r;k)=N_k^{(r)}(2\nu)^{-(k+r)}, \tag{6.9}$$

where $N_k^{(r)}$ is the number of first-entry, order-k preimages of the target interval. Recall $N_0^{(r)}=1$ and $N_k^{(r)}$ is equal to 2^{k-1}

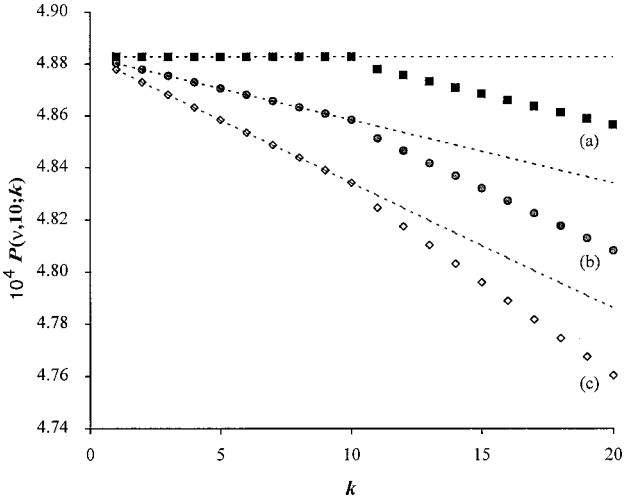

FIG. 7. Results of numerical calculations of $P(1+\epsilon,r;k)$ for $r=10$ when (a) $\epsilon=0$; (b) $\epsilon=5\times10^{-4}$; (c) $\epsilon=10^{-3}$. In each case the data that are unaffected by overlap are extrapolated as a dashed line in order to highlight the accelerated downward trend in $P(\nu,r;k)$ for $k>r$.

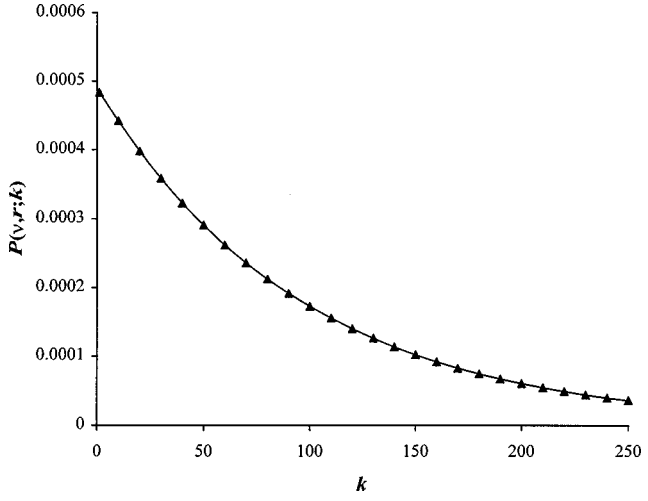

FIG. 8. Numerical calculations of $P(\nu,r;k)$ with $\nu=1.01$ and $r=10$, illustrating the k dependence of P for k in the range 1 to 250.

for $k=1,\ldots,r$, but for $k\geqslant r+1$, $N_k^{(r)}$ falls below 2^{k-1}, because of the overlap of some of these higher order first-entry pre-images with the target interval itself. In the absence of such corrections, Eq. (6.9) would take the form

$$\tilde{P}(\nu,r;k)=\begin{cases}(2\nu)^{-r}, & k=0\\ [(2\nu)^{-r}\nu^{-k}]/2, & k\geqslant 1.\end{cases} \tag{6.10}$$

Note that Eq. (6.10) includes the extrapolation of $\tilde{P}$ to values of k greater than r. While $\tilde{P}$ no longer provides an approximation to P for such values of k, the extrapolation is useful because the deviation of P from it represents the effect of preimage overlap. Thus,

$$P(\nu,r;k)\begin{cases}=\tilde{P}(\nu,r;k), & k=0,1,\ldots,r\\ <\tilde{P}(\nu,r;k), & k=r+1\ \ldots.\end{cases} \tag{6.11}$$

For $\nu>1$, Eq. (6.10) shows that $\tilde{P}(\nu,r;k)$ decreases as k increases. The rate of decrease is determined by $\epsilon=\nu-1$; the greater the value of ϵ, the more rapid the decline of $\tilde{P}(\nu,r;k)$ with k. Equation (6.11) shows that $P(\nu,r;k)$ follows the same downward trend as k increases from 1 to r, but thereafter the decline is accelerated by the reduction in the number of preimages contributing because of overlap. Figure 7 shows $P(1+\epsilon,10;k)$ and $\tilde{P}(1+\epsilon,10;k)$, with $\epsilon=0$, 5×10^{-4}, and 10^{-3}, for $k=1,\ldots,20$. The acceleration of the downward trend in the data for $P(\nu,r;k)$, arising from overlap, is clearly visible. However, this phenomenon is not always so obvious. The recurrence relation (3.10) can be used to show that the overlap correction

$$2^{r+j-1}-N_{r+j}^{(r)}=2^{j-1}+(j-1)2^{j-2}, \tag{6.12}$$

for $j=1,\ldots,r+1$. Observe that this correction does not depend explicitly on r. Thus, the greater the value of ϵ, the smaller are the first $r+1$ corrections due to overlap [since each is the difference given in Eq. (6.12) multiplied by the preimage length of $(2\nu)^{-(k+r)}$ with $k=r+j$]. These overlap corrections are also diminished at increased r. Not only do they first appear at larger values of k, but their value is also reduced by the r dependence of the preimage length while the preimage number deficits are still given by Eq. (6.12). As a consequence, the acceleration of the downward trend in $P(\nu,r;k)$ may not be as marked as that shown in Fig. 7 when ϵ is significantly greater than zero and/or larger values of r are used.

C. Asymptotic form for $P(\nu,r;k)$ at large k

1. Transient chaos

When $\nu>1$, the decline of $P(\nu,r;k)$ with increasing k is asymptotically exponential at large r with an exponent related to the escape rate κ. Figure 8 illustrates the exponential ''tail'' of $P(1+\epsilon,r;k)$ when $\epsilon=0.01$, $r=10$. The asymptotic form can be derived formally as follows. Equation (6.9) gives

$$\ln[P(\nu,r;k)]=\ln(N_k^{(r)})-k\ln 2-k\ln\nu-r\ln(2\nu) \tag{6.13}$$

and, therefore, the forward difference

$$\Delta\ln[P(\nu,r;k)]=\ln[P(\nu,r;k+1)])-\ln[P(\nu,r;k)]$$
$$=-\ln\nu+\ln\left[\frac{N_{k+1}^{(r)}}{2N_k^{(r)}}\right]. \tag{6.14}$$

For $k=1,\ldots,r-1$, the second term in (6.14) is zero because $N_{k+1}^{(r)}=2^k$ and $N_k^{(r)}=2^{k-1}$. However, for $k\geqslant r$, this term is affected by preimage overlap. An extension of the analysis of the recurrence relation (3.10) used to obtain Eq. (6.12) shows that

$$\frac{N_{r+j+1}^{(r)}}{2N_{r+j}^{(r)}}=1-2^{-(r+1)}+O(2^{-2(r+1)}), \tag{6.15}$$

for $j=0,1,\ldots,$ so that

$$\Delta \ln[P(\nu,r;r+j)] = -\ln \nu + \ln[1-2^{-(r+1)} + O(2^{-2(r+1)})]. \quad (6.16)$$

When r is large enough for the second term in the right-hand side of Eq. (6.16) to be neglected, it follows that

$$P(\nu,r;r+j+1) \approx P(\nu,r;r+j)\exp(-\kappa), \quad (6.17)$$

where $\kappa = \ln \nu$. Moreover, since Eq. (6.17) is true for any non-negative integer j, it follows that

$$P(\nu,r;r+n) \approx P(\nu,r;r)\exp(-\kappa n). \quad (6.18)$$

2. Permanent chaos

Equation (6.17) is based on the assumption that ν is bounded away from 1, i.e., $\nu = 1+\epsilon$ with $\epsilon > 0$, so that the large-r limit in Eq. (6.16) provides a nontrivial result. This assumption is made by Tél [4], and Eq. (6.18) gives the resulting asymptotic form that is dependent on the escape rate. However, it is clear that the crisis itself cannot be reached using the analysis of Sec. VI C 1. An alternative (and more practical) procedure is to recognize that there is a lower limit to the length of target interval that can be considered (corresponding to a maximum acceptable value of $r = r_*$), for otherwise the probability of success becomes unacceptably small, and to allow ν to approach 1 in Eq. (6.16) [or, more precisely, in Eq. (6.14)] with $r = r_*$. Under these circumstances, the first term in Eq. (6.16) becomes negligible compared with the second, so that

$$P(\nu,r_*;r_*+j+1) \approx P(\nu,r_*;r_*+j)\frac{N^{(r_*)}_{r_*+j+1}}{2N^{(r_*)}_{r_*+j}} \approx P(\nu,r_*;r_*+j)[1-2^{-(r_*+1)} + O(2^{-2(r_*+1)})], \quad (6.19)$$

and Eq. (6.18) is replaced by

$$P(\nu,r_*;r_*+n) \approx P(\nu,r_*;r_*)\prod_{j=1}^{n}\frac{N^{(r_*)}_{r_*+j+1}}{2N^{(r_*)}_{r_*+j}} \quad \text{(a)} \approx P(\nu,r_*;r_*)[1-2^{-(r_*+1)} + O(2^{-2(r_*+1)})]^n \quad \text{(b)}, \quad (6.20)$$

when $\nu = 1$ so that $\ln \nu = 0$, $\approx$ is replaced by $=$ in both Eqs. (6.20a,b). It is then clear [from Eq. (6.20a)] that the asymptotic behavior of $P(\nu,r_*;r_*+n)$ is determined by the numbers of preimages of the target interval that contribute to the event that the orbit first enters that interval in exactly $r+j$ iterations, with $j = 1,\ldots,n+1$. Moreover, Eq. (6.15) shows that the ratio $N^{(r)}_{r+j+1}/2N^{(r)}_{r+j}$ is independent of j to first order in $2^{-(r+1)}$, and therefore $P(\nu,r_*;r_*+n)$ depends only on n to this order [see Eq. (6.20b)].

3. Transitional behavior

The role played by the relative sizes of $\epsilon = \nu - 1 = \kappa + O(\epsilon^2)$, and $2^{-r} = \nu^r l(I_F) = \nu^{r-1} p_*$, in passing between Eqs. (6.18) and (6.20), can be obtained approximately by rewriting Eq. (6.16) as

$$\begin{aligned}\Delta \ln[P(\nu,r;r+j)] &= -\ln(1+\epsilon) + \ln[1-2^{-(r+1)} + O(2^{-2(r+1)})] \\ &\approx -\epsilon - 2^{-(r+1)} + O(\epsilon^2) + O(2^{-2(r+1)}), \\ &\approx -\kappa - \frac{1}{2}p_* + O(p_*\epsilon) + O(\epsilon^2) + O(2^{-2(r+1)}), \end{aligned} \quad (6.21)$$

for small ϵ and large r. Provided all but first-order terms in Eq. (6.21) can be neglected, it follows that

$$P(\nu,r;r+n) \approx P(\nu,r;r)\exp(-\kappa n)\exp(-\tfrac{1}{2}p_* n). \quad (6.22)$$

In this approximation, the ''escape'' ($\nu > 1, r \to \infty$) and ''overlap'' ($\nu \to 1, r \leqslant r_*$) mechanisms make independent contributions to the overall exponential tail of $P(\nu,r;k)$. This approximate independence of the escape and overlap mechanisms implies the existence of the transitional behavior in $\tau(\nu,r)$ that is shown in Fig. 6 (cf. Tél [4]).

VII. CONNECTION WITH THE CALCULATIONS OF Tél

Tél's calculations [4] are based on the assumption that the length of the target interval is so small that preimage overlap does not occur. It has been shown in Sec. VI that this assumption leads to the approximation (6.17) for $P(\nu,r;k)$ with $k > r$. This approximation is exact when $k = 1,\ldots,r-1$ and for $k = 0$ Eq. (6.14) gives

$$P(\nu,r;1) = P(\nu,r;0)(2\nu)^{-1}, \quad (7.1)$$

where $P(\nu,r;0) = (2\nu)^{-r}$. Thus, replacing k by n in order to match the notation of Tél [4], it follows that

$$P(\nu,r;n)\begin{cases} = P(\nu,r;1)\exp[-\kappa(n-1)], & n = 1,\ldots,r \\ \approx P(\nu,r;1)\exp[-\kappa(n-1)], & n = r+1,\ldots \end{cases} \quad (7.2)$$

and

$$\sum_{n=0}^{\infty} P(\nu,r;n) \approx (2\nu)^{-r} + \frac{(2\nu)^{-r}}{(2\nu)}\sum_{n=1}^{\infty}\exp[-\kappa(n-1)] \approx \Delta_0 + \Delta_1[1-\exp(-\kappa)]^{-1}, \quad (7.3)$$

where $\Delta_0 = (2\nu)^{-r} = P(\nu,r;0)$ and $\Delta_1 = (2\nu)^{-r}/(2\nu) = P(\nu,r;1)$. This result is equivalent to Eq. (4) in [4]. Note that it is a feature of the symbolic approach to OGY control that Δ_0 and Δ_1 depend on ν. However, as $\nu \to 1$ both parameters simply increase monotonically to their ($\nu = 1$) values of 2^{-r} and $2^{-(r+1)}$, respectively. Also notice that the above definition of Δ_0 differs from that used in [4] by a factor of 2ν. In the present work, the term Δ_0 arises from the event

that the initial point is chosen in the target interval itself, when the control would be applied immediately. The formulation of the problem used in [4] counts those points that are controlled in one or more iterations.

The result corresponding to Eq. (5) of [4] follows from

$$\sum_{n=1}^{\infty} nP(\nu,r;n) \approx \Delta_1 \sum_{n=1}^{\infty} n\exp[-\kappa(n-1)] \approx \Delta_1[1-\exp(-\kappa)]^{-2}, \tag{7.4}$$

and the average number of iterations to achieve control, τ is given by

$$\tau = \frac{\sum_{n=1}^{\infty} nP(\nu,r;n)}{\sum_{n=0}^{\infty} P(\nu,r;n)} \approx \frac{\Delta_1[1-\exp(-\kappa)]^{-2}}{\Delta_0+\Delta_1[1-\exp(-\kappa)]^{-1}}. \tag{7.5}$$

Following [4], consider $\kappa \ll 1$. It is straightforward to argue that $[1-\exp(-\kappa)]^{-1} \gg 1$ so that

$$\tau \approx [1-\exp(-\kappa)]^{-1} = [\kappa + O(\kappa^2)]^{-1} \approx \kappa^{-1}. \tag{7.6}$$

However, it is important to realize that the denominator in Eq. (7.5) does not diverge as κ tends to zero: in fact, it must itself tend to zero in this limit.

In order to neglect corrections arising from preimage overlap, it was necessary to assume that $\nu - 1 = \epsilon \gg 2^{-(r+1)}$ [cf. Eq. (6.21)] and the validity of Eq. (7.5) depends on this condition being maintained. Since $2^{-(r+1)} > \Delta_1$ and $\kappa = \ln(1+\epsilon) \approx \epsilon$, it follows that $\Delta_1 \ll \kappa$ is obligatory when the approximation in Eq. (7.5) is used. Thus, there is no question of the denominator in Eq. (7.5) diverging; rather, it tends to zero as κ approaches zero. The condition $\Delta_1 \ll \kappa$ must be ensured by reducing the length of the target interval (or, equivalently, increasing r) to avoid preimage overlap. For small κ, $\Delta_0 \ll \Delta_1 \kappa^{-1}$ and, as $\kappa \to 0$, the denominator in Eq. (7.5) tends to zero. This behavior is consistent with Eqs. (4.3) and (6.8), which show that the probability of successful control tends to zero as r tends to infinity.

VIII. CONCLUSION

The usual formulation of the symbolic dynamics of a tent map given by Eq. (2.1) provides a symbolic labeling of the preimages of a class of intervals that converge onto its nontrivial fixed point. Provided that the target interval is chosen in this class, the problem of OGY control to the fixed point can be reduced to an equivalent combinatorial problem involving the numbers of binary strings of finite length that have the target symbol block only at their right-hand end. This string counting problem has been solved by established techniques to obtain the recurrence relation and the generating function for the numbers of preimages of the target interval contributing to OGY control. The difficulties of preimage overlap noted by Tél [4] are dealt with exactly in this formulation of the problem. The recurrence relation allows the probability $p_n(\nu,r)$ of achieving control in less than or equal to n iterations to be calculated, while the generating function leads to closed forms for both the probability $p(\nu,r)$ of successful control and the average number $\tau(\nu,r)$ of iterations to control when it occurs.

The results obtained in this paper confirm the pioneering work of Tél [4] and extend it by providing an exact solution to the problem of OGY control of transient chaotic behavior in the special case of the family of tent maps (1.2). In the present work (as in Tél [4]) attention has been focused on achieving control by stabilization of the nontrivial fixed point of the maps, but the symbolic approach presented here is not limited to that case. The symbolic formulation of OGY control to a periodic orbit of nontrivial period for tent maps near crisis, and its solution, will be discussed in the following paper [14].

[1] W. Ditto and T. Munakata, Commun. ACM **38**, 96 (1995).

[2] E. Ott, C. Grebogi, and J.A. Yorke, Phys. Rev. Lett. **64**, 1196 (1990).

[3] G. Chen and X. Dong, *From Chaos to Order* (World Scientific, Singapore, 1998).

[4] T. Tél, J. Phys. A **24**, L1359 (1991).

[5] T. Tél, in *STATPHYS'19*, edited by Hao Bai-Lin (World Scientific, Singapore, 1996), pp. 346–362.

[6] C. Beck and F. Schlögl, *Thermodynamics of Chaotic Systems* (Cambridge University Press, Cambridge, 1993).

[7] C. Grebogi, E. Ott, and J.A. Yorke, Phys. Rev. Lett. **48**, 1507 (1982).

[8] D.K. Arrowsmith and C.M. Place, *Dynamical Systems* (Chapman & Hall, London, 1992).

[9] J. Guckenheimer, G. Oster, and A. Ipaktchi, J. Math. Biol. **4**, 101 (1977).

[10] A.M. Odlyzko, in *Handbook of Combinatorics*, edited by R.L. Graham, M. Grötschel, and L. Lovász, (Elsevier, Amsterdam, 1995), Vol. 2, Chap. 22.

[11] G.H. Hardy, *An Introduction to the Theory of Numbers* (Oxford University Press, Oxford, 1979).

[12] C.M. Place and D.K. Arrowsmith, Interim Report, Mathematics Research Centre, School of Mathematical Sciences, Queen Mary & Westfield College, London (unpublished).

[13] T. Tél, Phys. Rev. A **36**, 1502 (1987).

[14] C.M. Place and D.K. Arrowsmith, following paper, Phys. Rev. E **61**, 1369 (2000).